

Effect of a magnetic field on Ni-Pt alloys

Dilip Kumar Saha and Ken-ichi Ohshima

Institute of Applied Physics, University of Tsukuba, Tsukuba 305, Japan

(Received 26 July 1994; revised manuscript received 18 October 1994)

Magnetic properties of $\text{Ni}_{1-x}\text{Pt}_x$ alloys were studied in both the disordered and ordered states for $x=0.25, 0.35, 0.44,$ and 0.50 . Different magnetic fields were applied in the range from 0 to 800 Oe for the disordered state and from 0 to 10 kOe for the ordered state under the zero-field cooling condition with the temperature range from 5 to 400 K. For $x=0.25$ and 0.35 alloys, a ferromagnetic moment was observed in both the disordered and ordered states for the whole magnetic-field range. In the ordered state, an unusual behavior of the magnetic moment was observed, which is independent of magnetic field. For the $x=0.44$ alloy, a ferromagnetic moment was observed in the disordered state, but peculiar results were observed in the ordered state. A weak ferromagnetic moment appeared at 0 and 10 Oe magnetic field but from 50 up to 1000 Oe magnetic field, an antiferromagnetic-type feature is seen, where the antiferromagnetic-paramagnetic transition temperature T_N decreases monotonically with increasing magnetic field. Further, from 1200 Oe up to 10 kOe, the paramagnetism is evident. Hysteresis-loop data and the curve of the inverse of the magnetic susceptibility confirmed antiferromagnetism in the alloy. This is the first observation to our knowledge for such a change under an applied magnetic field in the binary alloys. For the $x=0.50$ alloy, a ferromagnetic moment in the disordered state and a clear paramagnetic moment in the ordered state were observed for the whole magnetic-field range.

I. INTRODUCTION

$3d$ ferromagnetic metal-based alloys are technologically important because of their favorable mechanical properties and peculiar magnetic moment. In recent years work has been done on the magnetic properties for systems such as Ni-Rh, Ni-Mn, Fe-Pt, Co-Pt.¹⁻⁴ In the Ni-Pt alloy system, work on magnetic properties and spatial order had been done by Cadeville, Dahmani, and Kern.⁴ They determined a partial magnetic phase diagram for this alloy system. Though they observed the disappearance of the magnetic moment in the ordered state of $\text{Ni}_{1-x}\text{Pt}_x$ alloys between $x=0.44$ and 0.60 , they did not study detailed magnetic properties in this alloy system. On the other hand, in the Ni-Pt alloy phase diagram, there are two ordered structures below the order-disorder transition temperature, T_p . Figure 1 shows the partial atomic phase diagram, where $L1_2$ -type (Cu_3Au) and $L1_0$ -type (CuAu) ordered structures exist in the com-

position ranges from $x=0.18$ to 0.35 and from $x=0.36$ to 0.75 , respectively.⁵ $L1_0$ is a layered structure along the c axis with tetragonal symmetry but $L1_2$ has a cubic symmetry. Above T_p , Ni-Pt has the fcc structure in the whole composition range. Ferromagnetism occurs at 361°C for pure Ni and its transformation temperature gradually decreases with increasing Pt content up to about $x=0.27$, where the transformation temperature is 100°C . Dahmani, Cadeville, and Bohnes⁶ measured the temperature dependence of atomic relaxation times for both the ordered and disordered states in the Ni-Pt system. They observed an important slowing down effect in the vicinity of the order-disorder phase transition. There are no other reports on magnetization for the Ni-Pt system.

It is, therefore, of great interest to understand the effect of applied magnetic field on the magnetic moment, both in the ordered and disordered states, in the Ni-Pt alloy system. In this paper, we present our experimental data, which were taken from both the ordered and disordered states at different applied magnetic fields and without magnetic field under the ZFC condition. In some cases hysteresis-loop curves will also be presented. New and peculiar results were observed in some samples, where the spin and magnetic moment changes with applied magnetic field.

II. EXPERIMENT

Four polycrystalline samples were prepared by melting 99.999% pure Ni and 99.99% pure Pt using an arc-melting furnace in an argon atmosphere. Subsequently, the alloys were remelted nine to ten times to homogenize the specimens. The sample ingots were cut into two different shapes; a rectangular shape for magnetic mea-

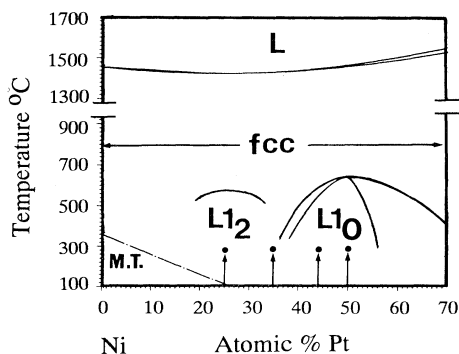


FIG. 1. Partial atomic phase diagram of the Ni-Pt alloy system.

surement with dimensions of $6 \times 4 \times 3 \text{ mm}^3$ and a strip shape which was cut from thin rolled sheet for x-ray Debye-Scherrer experiments. After heat treatment of the samples above T_p to remove strain, the lattice parameters of the quenched specimens in the disordered state were measured with an x-ray Debye-Scherrer camera using Cu $K\alpha$ radiation. The specimen compositions were determined with an accuracy of $\pm 0.3 \text{ at. \%}$ by comparison with the lattice parameter versus composition relation.⁷ The four compositions were determined as $x=0.25, 0.35, 0.44,$ and 0.50 in $\text{Ni}_{1-x}\text{Pt}_x$ alloys. The compositions of the alloys were selected in such a way that they will cover two different regions of ordered structure. In Fig. 1, arrows and dots indicate the positions of the four different compositions in the phase diagram. For magnetic measurements, all the samples were annealed separately in evacuated silica tubes at 1000°C for 4 days, 900°C for 1 day, and 850°C for 5 days successively and quenched by dropping into ice water. It was confirmed by x-ray experiments that the state of the specimens was disordered. A superconducting quantum interference device (SQUID) was used to determine the following magnetic parameters; (1) spontaneous magnetic moment, $M_S(T_c)$; (2) ferromagnetic-paramagnetic transition temperature, T_c ; (3) magnetic susceptibility at the transition temperature, $\chi(T_c)$; (4) the deviating temperature (from the Curie-Weiss law), T_0 ; (5) temperature, T_x , from the Curie-Weiss law of inverse of the susceptibility curve where the straight line touches the horizontal axis; (6) Curie constant, C ; and (7) the effective number of Bohr magneton, p_{eff} . All the data were taken in the temperature range $5\text{--}400 \text{ K}$ with and without applied magnetic field. Four different magnetic fields of $0, 100, 400,$ and 800 Oe were applied at low temperature after zero-field cooling (ZFC).

Next heat treatment was done for all the four samples separately in evacuated silica tubes at 500°C for 15 days continuously and then slowly cooled down at room temperature within the next 5 days to obtain the ordered state of the specimens. For the $x=0.35$ sample, heat treatment was done from 350°C due to the low value of T_p . To confirm the ordered state of the specimens, x-ray Debye-Scherrer experiments were conducted, where the c/a ratio was observed to be 0.944 and 0.940 for the $x=0.44$ and 0.50 alloys, respectively. These results are in good agreement with literature values of 0.942 and 0.939 , respectively.⁷ Superlattice peaks confirmed the specimen with $x=0.25$ is perfectly ordered. Magnetic measurements were done in the ordered state and all the magnetic

parameters were determined, using the ZFC condition in the temperature range from 5 to 400 K with and without magnetic field. Different magnetic fields were applied in the range from 0 to 10 kOe at low temperature after ZFC. In three samples, a hysteresis-loop experiment was done at different fixed temperatures with the applied magnetic field in the range from -3 to $+3 \text{ T}$ to confirm their peculiar magnetic properties. In addition to the magnetic properties of the disordered state, we have determined the antiferromagnetic-paramagnetic transition temperature, T_N , and the paramagnetic Curie temperature, Θ , from the ordered state of the same $x=0.44$ sample.

III. RESULTS AND DISCUSSION

A. Disordered state

Figures 2(a)–2(d) show the magnetic moment, M (emu/g), versus temperature, $T(\text{K})$, plots (warming curves) at $H=0$ and 800 Oe for $x=0.25, 0.35, 0.44,$ and 0.50 in $\text{Ni}_{1-x}\text{Pt}_x$ alloys, respectively. Figures 2(a) and 2(b) indicate clear ferromagnetic-type magnetic moments and the nature of the magnetic-moment curves are similar for both cases. Spontaneous magnetization sharply vanishes just after T_c in the zero magnetic field ($H=0 \text{ Oe}$) condition. It is clear that below T_c each specimen shows ferromagnetism and above T_c they show paramagnetism. The flatness of spontaneous magnetization against temperature decreases with increasing magnetic field. At a magnetic field of 800 Oe , a decrease of spontaneous magnetization with decreasing temperature, starting from T_c , was observed for both alloys. All the curves of Figs. 2(c) and 2(d) show the ferromagnetic-type magnetization. The change of magnetic moment around T_c becomes smooth with increasing applied magnetic field. This fact means that the paramagnetic interaction is getting preference over the ferromagnetic interaction.

We have summarized spontaneous magnetization, $M_S(T_c)$ and $\chi(T_c)$ at T_c in Table I for all four samples. In Table I, we see that the ferromagnetic spontaneous magnetization, M_S (emu/g), shows a continuous increase with increasing magnetic field. The M_S values for the $x=0.25$ and 0.35 alloys are almost the same, but slightly lower values were observed for the $x=0.44$ and 0.50 alloys. We also see that the magnetic susceptibility χ (emu/g Oe) decreases with increasing applied magnetic field for all four specimens. Both the χ values and m_s

TABLE I. Ferromagnetic spontaneous magnetic moment, $M_S(T_c)$, and susceptibility, $\chi(T_c)$, at different applied magnetic fields for all four samples in the disordered state.

| Applied magnetic field (Oe) | $x=0.25$ | | $x=0.35$ | | $x=0.44$ | | $x=0.50$ | |
|-----------------------------|--------------------|---|--------------------|---|--------------------|---|--------------------|---|
| | $M_S(T_c)$ (emu/g) | $\chi(T_c)$ (emu/g Oe) $\times 10^{-3}$ | $M_S(T_c)$ (emu/g) | $\chi(T_c)$ (emu/g Oe) $\times 10^{-3}$ | $M_S(T_c)$ (emu/g) | $\chi(T_c)$ (emu/g Oe) $\times 10^{-3}$ | $M_S(T_c)$ (emu/g) | $\chi(T_c)$ (emu/g Oe) $\times 10^{-3}$ |
| 0 | 0.30 | | 0.09 | | 0.46 | | 0.40 | |
| 100 | 3.10 | 31.0 | 3.00 | 30.0 | 2.50 | 25.0 | 1.60 | 16.0 |
| 400 | 9.20 | 23.0 | 9.10 | 22.8 | 7.50 | 18.8 | 4.80 | 12.0 |
| 800 | 10.00 | 12.5 | 10.00 | 12.5 | 9.20 | 11.5 | 5.50 | 6.9 |

values tend to decrease with increasing Pt content for the different applied magnetic fields. Pure Ni is strongly ferromagnetic but pure Pt is paramagnetic. Therefore, the alloys of the Ni-Pt system have a tendency to show a decrease of the ferromagnetic moment with increasing Pt content.

Table II presents the values of T_c , T_0 , T_x , C , and p_{eff} for all four samples in the disordered state. The 400-Oe data were used to calculate all the values in Table II except for T_c , which was taken from the zero applied magnetic field curve. The value of T_c is almost constant with applied magnetic field but continuously decreases with in-

creasing Pt content in the alloys. The values of T_c listed in Table II are in good agreement with Ref. 4 values. The inverse of susceptibility ($1/\chi$) versus temperature curve was plotted to calculate T_0 and T_x . A continuous decrease of T_0 with increasing Pt content was observed except for $x=0.50$. The value of T_x was observed which decreases continuously with increasing Pt content. The positive sign of T_x for all cases indicates that the ferromagnetic interactions have more influence on the Ni spin bonds in the crystal and that the influence decreases with increasing Pt content in the alloys. To calculate the Curie constant, C , and the effective number of Bohr mag-

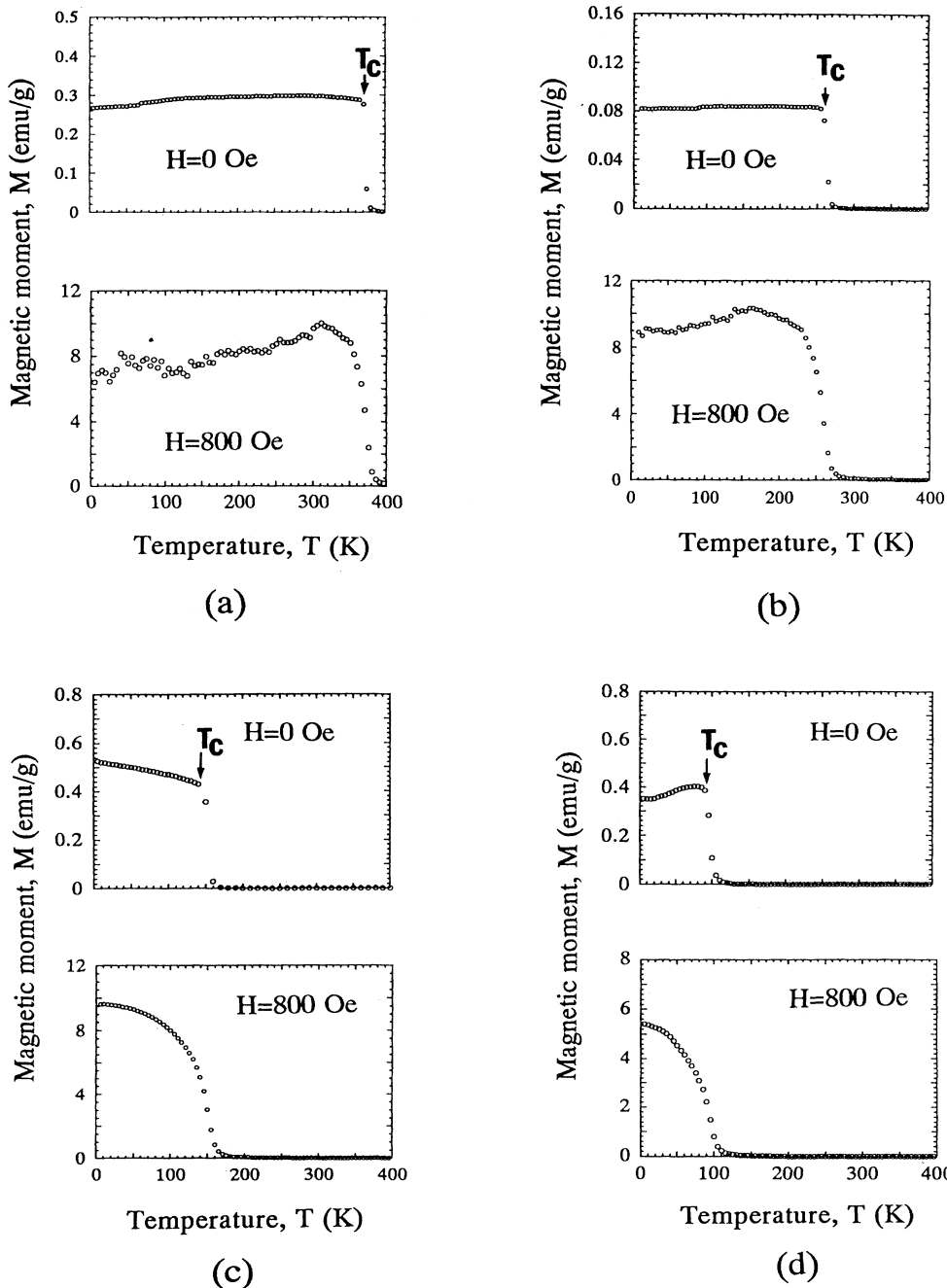


FIG. 2. dc magnetic moment, M , vs temperature, T , plots in the disordered state for (a) $x=0.25$, (b) $x=0.35$, (c) $x=0.44$, and (d) $x=0.50$ in $\text{Ni}_{1-x}\text{Pt}_x$ alloys. Different magnetic fields were applied at low temperature after the zero-field-cooling (ZFC) condition (warming curves).

TABLE II. All the values of T_c , T_0 , T_x , C , and p_{eff} for all four samples in the disordered state.

| x value in $\text{Ni}_{1-x}\text{Pt}_x$ | T_c (K) | T_0 (K) | T_x (K) | C (10^{-3} emu/g Oe)K | p_{eff} (μ_B) |
|--|--------------|--------------|--------------|-------------------------------|---------------------------------|
| 0.25 | 370±5 | 385±5 | 378±5 | 5.32 | 0.206 |
| 0.35 | 255±5 | 325±5 | 276±5 | 4.22 | 0.184 |
| 0.44 | 140±5 | 235±5 | 170±5 | 3.34 | 0.164 |
| 0.50 | 90±5 | 310±5 | 152±5 | 1.94 | 0.119 |

neton p_{eff} , $C = \chi(T - T_c)$ and $p_{\text{eff}} = [3Ck_B/N]/\mu_B$ were used, respectively, where the value of χ was taken from the higher-temperature region ($T > T_0$). The constant values k_B , N , and μ_B are the Boltzmann constant, Avogadro's number, and Bohr magneton, respectively. The values of p_{eff} in μ_B decrease with increasing Pt content, indicating that Ni has a higher magnetic moment than Pt.

B. Ordered state

Figures 3(a)–3(d) show the magnetic moment versus temperature plots (warming curves) at $H=0, 400$, and 2 kOe for $x=0.25, 0.35, 0.44$, and 0.50 in $\text{Ni}_{1-x}\text{Pt}_x$ alloys, respectively. We have observed different characteristics of the magnetic moment in the ordered state from those for the disordered state. Figures 3(a) and 3(b) indicate a ferromagnetic-type magnetic moment for $x=0.25$ and 0.35 , respectively. An unstable magnetic moment appears in the ferromagnetic part of the magnetization

curve starting from the 100-Oe applied magnetic field. This instability increases with increasing magnetic field. At high magnetic field (400 Oe and above), a peak developed near T_c for the $x=0.35$ alloy, indicating the tendency for a change of magnetic moment from ferromagnetic to antiferromagnetic-type. This type of change was not observed in the disordered state of the same alloy.

In Figs. 3(c) and 3(d), we have observed completely different characteristics of magnetic moment in the ordered state compared with those for the disordered state. In Fig. 3(c), a very weak ferromagnetic moment without any spontaneous magnetization was observed at zero magnetic field, but at 400 Oe, the antiferromagnetic peak exists. At 2 kOe, a weak paramagnetic moment appears with complete disappearance of the antiferromagnetic peak. This is the first time we have observed such a peculiar type of change of magnetic moment in a binary alloy system, where spin direction and the nature of the magnetic moment changes with magnetic field. Figure 3(d)

TABLE III. Ferromagnetic spontaneous magnetic moment, $M_S(T_c)$, and magnetic susceptibility, $\chi(T_c)$, for $x=0.25$ and 0.35 in $\text{Ni}_{1-x}\text{Pt}_x$ alloys and the antiferromagnetic-paramagnetic transition temperature, T_N , $M(T_5)$, and susceptibility, $\chi(T_N)$, for the $x=0.44$ alloy and $M(T_5)$, and $\chi(T_5)$ for the $x=0.50$ alloy in the ordered state. T_5 means the temperature at 5 K.

| Applied magnetic field (Oe) | $x=0.25$ | | $x=0.35$ | | $x=0.50$ | |
|-----------------------------|--------------------|---|-----------------------------------|---|--------------------|---|
| | $M_S(T_c)$ (emu/g) | $\chi(T_c)$ (emu/g Oe) $\times 10^{-3}$ | $M_S(T_c)$ (emu/g) | $\chi(T_c)$ (emu/g Oe) $\times 10^{-3}$ | $M_S(T_5)$ (emu/g) | $\chi(T_5)$ (emu/g Oe) $\times 10^{-3}$ |
| 0 | 0.32 | | 0.35 | | 0.18 | |
| 100 | 2.10 | 21.00 | 1.70 | 17.00 | 1.35 | 13.50 |
| 400 | 2.30 | 5.80 | 1.80 | 4.50 | 5.80 | 14.50 |
| 800 | 2.30 | 2.90 | 1.90 | 2.40 | 12.00 | 15.00 |
| 2 K | 2.30 | 1.20 | 2.00 | 1.00 | 30.00 | 15.00 |
| 10 K | 2.30 | 0.23 | 1.70 | 0.17 | 133.00 | 13.30 |
| Applied magnetic field (Oe) | T_N (K) | $x=0.44$ | | | | |
| | | $M(T_5)$ (emu/g) | $\chi(T_N)$ (10^{-4} emu/g Oe) | | | |
| 0 | | 0.110 | | | | |
| 10 | | 0.310 | | | | |
| 50 | 42 | 0.120 | 7.00 | | | |
| 100 | 40 | 0.042 | 6.50 | | | |
| 400 | 30 | 0.040 | 4.80 | | | |
| 800 | 20 | 0.170 | 3.50 | | | |
| 1 K | 12 | 0.320 | 3.45 | | | |
| 2 K | | 0.500 | | | | |
| 10 K | | 0.820 | | | | |

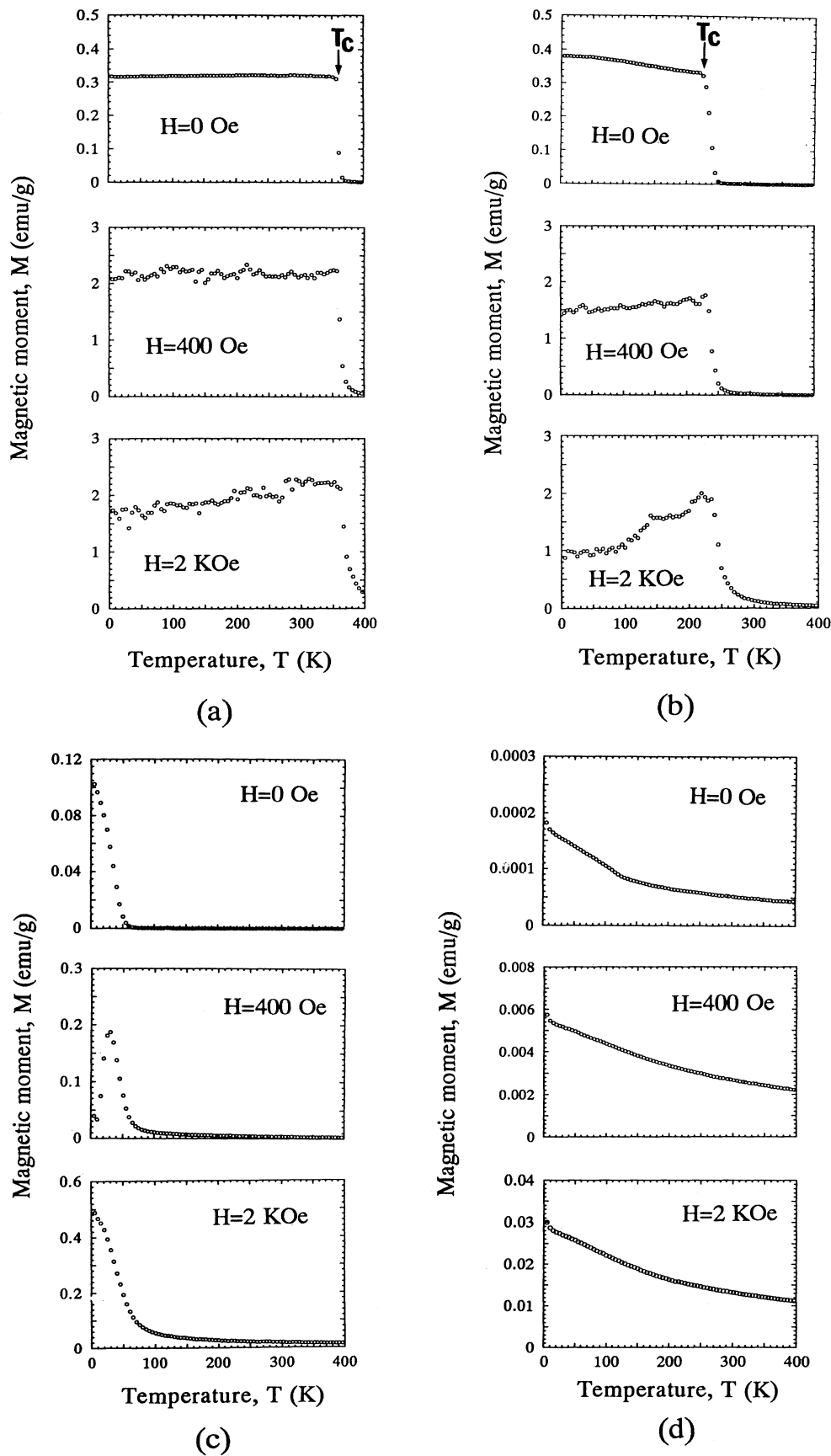


FIG. 3. dc magnetic moment, M , vs temperature, T , plots in the ordered state for (a) $x=0.25$, (b) $x=0.35$, (c) $x=0.44$, and (d) $x=0.50$ in $\text{Ni}_{1-x}\text{Pt}_x$ alloys. Different magnetic fields were applied at low temperature after the ZFC condition (warming curves).

shows a magnetic moment for the $x=0.50$ alloy. We have observed a clear paramagnetic moment for this alloy in the ordered state although a ferromagnetic moment was observed in the disordered state for the whole range of magnetic field. To discover where the antiferromagnetic peak appears and where it disappears for the $x=0.44$ alloy, we have taken a series of magnetic moment data for extra applied magnetic fields as shown in Fig. 4. We see that even at 10 Oe, a weak ferromagnetic moment exists having larger moment value than that for zero applied field at 5 K. At 50 Oe, a weak antiferromagnetic peak appears at 42 K, though a decrease of ferromagnetic moment at 5 K was observed compared with the value of 10 Oe. At 1000 Oe, the peak shows a perfectly antiferromagnetic-type moment like Pd-Mn alloys.⁸ Above 1200 Oe, there is no existence of an antiferromagnetic moment.

All the data for the ordered state of the four samples are summarized in Tables III and IV. In Table III, we see that the spontaneous magnetic moment M_S at T_c in emu/g is almost constant for the whole magnetic field range for $x=0.25$ and 0.35 alloys. This is peculiar behavior for the ferromagnetic moment because normally the magnetic moment increases with increasing magnetic field. As the ferromagnetic spins of Ni atoms are thought to be frozen due to the ordering process, Ni spins do not respond with magnetic field and we have observed constant magnetic moment with magnetic field. For $x=0.44$ and 0.50 alloys, we have observed a much lower magnetic moment $M(T_5)$, in the ordered state than that for the disordered state, where $T_5=5$ K, starting temperature. The $x=0.44$ and 0.50 alloys have no T_c due to the absence of a ferromagnetic moment (Table IV). But certain cases for the $x=0.44$ alloy exhibit an antiferromagnetic-paramagnetic transition temperature, T_N , and that value decreases from 42 K down to 12 K with increasing magnetic field from 50 to 1000 Oe. So we have summarized $M(T_5)$ and $\chi(T_5)$ for the $x=0.44$ alloy and $M(T_5)$ and $\chi(T_N)$ for the $x=0.50$ alloy instead of $M_S(T_c)$ and $\chi(T_c)$. The magnetic moment at 5 K first increases then decreases and again increases with increasing magnetic field for the $x=0.44$ alloy. For $x=0.50$, a continuous increase of moment with increasing magnetic field was observed at 5 K although the absolute values are very small. A continuous decrease of magnetic susceptibility was observed with increasing magnetic field for $x=0.25$ and 0.35 alloys, but for the $x=0.44$ alloy, magnetic susceptibility, $\chi(T_N)$, decreases slightly with increasing magnetic field. For the $x=0.50$ alloy, almost constant susceptibility $\chi(T_5)$ was observed with increasing magnetic field. This

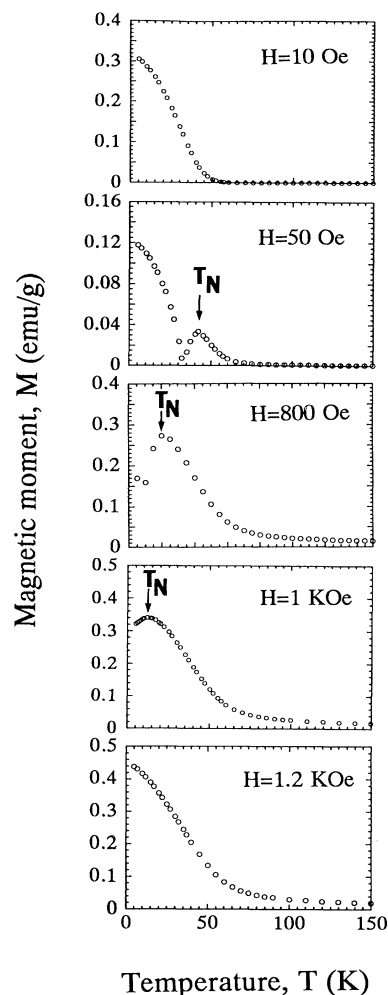


FIG. 4. dc magnetic moment, M , vs temperature, T , plots in the ordered state for the $x=0.44$ alloy. Different magnetic fields were applied to discover the appearance and disappearance of the antiferromagnetic peak.

is a good example of a paramagnetic moment in the $x=0.50$ alloy.

Table IV shows the values of T_c , T_0 , T_x , C , and p_{eff} for all samples in the ordered state. The 400-Oe data were used to calculate all the parameters except for T_c (T_c being taken from zero applied magnetic field data, by definition). Similar trends of decrease of T_c with increas-

TABLE IV. All the values of T_c , T_0 , T_x , Θ , C , and p_{eff} for all four samples in the ordered state.

| x value in $\text{Ni}_{1-x}\text{Pt}_x$ | T_c (K) | T_0 (K) | T_x (K) | Θ (K) | C (10^{-3} emu/g Oe) K | p_{eff} (μ_B) |
|--|--------------|--------------|--------------|-----------------|--------------------------------|---------------------------------|
| 0.25 | 355 ± 5 | 370 ± 5 | 365 ± 5 | | 5.59 | 0.212 |
| 0.35 | 225 ± 5 | 305 ± 5 | 250 ± 5 | | 4.01 | 0.179 |
| 0.44 | | 245 ± 5 | | -47 ± 5 | 2.50 | 0.142 |
| 0.50 | | 270 ± 5 | | -168 ± 5 | 2.03 | 0.127 |

ing Pt content were observed for $x=0.25$ and 0.35 alloys, like those for the disordered state. But almost constant values of T_c with applied magnetic field were observed for both alloys. The $x=0.44$ and 0.50 alloys have no T_c due to the absence of a ferromagnetic moment. We have observed slightly lower T_0 values for $x=0.25$, 0.35 , and 0.50 alloys in the ordered state compared with the disordered state. But a slightly higher value of T_0 was observed for the $x=0.44$ alloy in the ordered state compared with the disordered state. T_x is positive for $x=0.25$ and 0.35 alloys but negative for $x=0.44$ and 0.50 alloys, and is called the paramagnetic Curie temperature, Θ , with values of -47 and -168 K, respectively. This is a good example of an antiferromagnetic-type moment, for the $x=0.44$ alloy, like Pd-Mn.⁸ For the $x=0.50$ alloy, the value of Θ is -168 K in the ordered state compared with the disordered-state value of 152 K (T_x). This negative and higher value of Θ indicates that the sample contains a flat area of paramagnetic moment in the disordered state. Due to different types of magnetic moment in the ordered state, $C=\chi(T-T_c)$ was considered for $x=0.25$ and 0.35 alloys, but $C=\chi(T+\Theta)$ and $C=\chi T$ were considered for $x=0.44$ and 0.50 alloys, respectively, in calculating the C value. For all cases, the value of χ was taken from the higher temperature region ($T > T_0$). The same disordered-state equation was used for all samples to calculate the p_{eff} value. The value of C and p_{eff} are almost the same both in the ordered and disordered states for the $x=0.25$, 0.35 , and 0.50 alloys. But for the $x=0.44$ alloy, lower values of C and p_{eff} were observed in the ordered state compared with the disordered state.

C. Hysteresis loop (M - H curve)

To confirm the peculiar antiferromagnetic and paramagnetic moments in the ordered state of the

$x=0.44$ alloy, we have performed a hysteresis-loop experiment at four different temperatures (5 , 20 , 40 , and 100 K) within the magnetic field range from -3 to $+3$ T. The sequence of applied magnetic field was from 0 to $+3$ T, then from $+3$ T back to 0 again, from 0 to -3 T, then from -3 T back to 0 . Figure 5(a) shows some hysteresis-loop (for 5 , 40 , and 100 K) plots for the $x=0.44$ alloy. The nature of the loop for 5 , 20 , and 40 K is an antiferromagnetic type with a weak ferromagnetic moment. Marchukov *et al.*⁹ have recently measured M - H curves of $\text{Ca}_2\text{Fe}_2\text{O}_5$ at 20 K, this system showing an antiferromagnetic-type moment with a weak ferromagnetic moment. Their data are very similar to the present data for 20 and 40 K. At 100 K, the loop is just like a paramagnetic type. The anomaly in the low magnetic field region for 5 -K data is due to the presence of a ferromagnetic moment at low temperature, and its peculiar change with magnetic field (see data in Table III). For the $x=0.25$ and 0.50 alloys, another two sets of loop data were taken to compare results with those for the $x=0.44$ alloy, which were shown in Figs. 5(b) and 5(c), respectively, at temperature of 90 K with the same applied magnetic field range and sequence as was used for the $x=0.44$ alloy. Good agreement was observed with the ferromagnetic-type loop for $x=0.25$ alloy and with the paramagnetic-type loop for $x=0.50$ alloy. The peculiar shape for the $x=0.25$ alloy is due to the fixed value of magnetic moment with increasing magnetic field.

D. Partial magnetic phase diagram

Figure 6 shows the partial magnetic phase diagram which was constructed from the present SQUID data. In the atomic disordered state, the ferromagnetic-paramagnetic transition temperature, T_c , decreases linearly with increasing Pt content in the alloys. In the

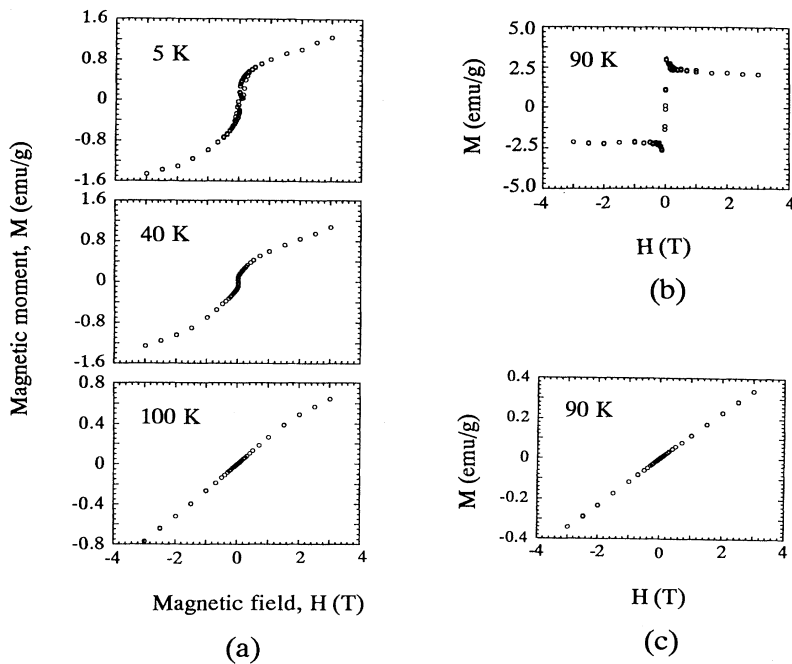


FIG. 5. Hysteresis-loop (magnetic field versus moment) plots in the ordered state for (a) $x=0.44$, (b) $x=0.25$, and (c) $x=0.50$ in $\text{Ni}_{1-x}\text{Pt}_x$ alloys.

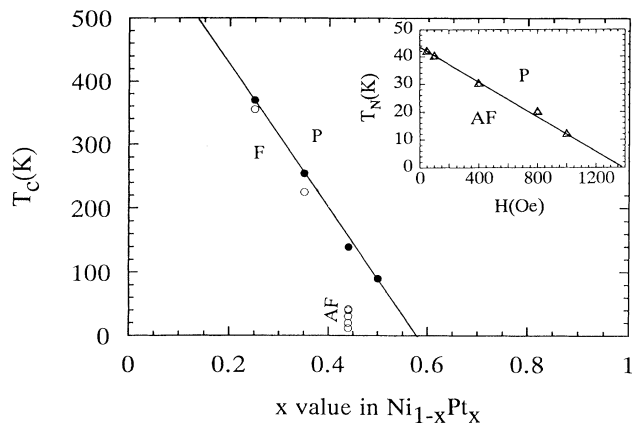


FIG. 6. Partial magnetic phase diagram of Ni-Pt alloys using a SQUID both from atomic disordered and ordered states. (●) Atomic disordered state data, (○) atomic ordered state data. Inset: magnetic-field dependency phase diagram for the $x=0.44$ alloy.

atomic ordered state, a new phase was observed for the $x=0.44$ alloy, where the phase transition occurs with applied magnetic field. An antiferromagnetic-paramagnetic phase transition was observed between the applied magnetic field of 50 and 1000 Oe. The antiferromagnetic-paramagnetic transition temperature, T_N , is also linear as shown in the inset of Fig. 6. This is a completely new phase in the binary alloy system. Extrapolation of the line indicates that the T_N value for the 1200-Oe magnetic field is 6 K. Our starting temperature was 5 K, so we could not see any antiferromagnetic peak in the plot for the 1200-Oe magnetic field. The extrapolated line indicates that the zero value of T_N occurs for a magnetic field of 1400 Oe.

IV. SUMMARY

The main purpose of this study was to understand the effect of applied magnetic field in both the ordered and disordered states for four alloys of $x=0.25, 0.35, 0.44$, and 0.50 in $\text{Ni}_{1-x}\text{Pt}_x$. Different magnetic fields were applied in the range from 0 to 800 Oe in the disordered state and from 0 to 10 kOe in the ordered state under the ZFC condition within the temperature range from 5 to 400 K. The following remarkable results were observed from the study.

(1) For $x=0.25$ and 0.35 alloys, a ferromagnetic moment was observed in both the ordered and disordered states for the whole magnetic-field range. In the disordered state, a continuous increase of magnetic moment was observed with increasing magnetic field for both alloys, which indicates normal magnetic behavior. But in the ordered state, an almost constant magnetic moment was observed with increasing magnetic field after 100 Oe for both alloys. Due to this independent magnetic moment with magnetic field, we have observed a peculiar shape in the hysteresis loop for the $x=0.25$ alloy. This is completely unusual behavior for magnetic moment in the alloys. The disordered state has the fcc structure but the

ordered state has the $L1_2$ -type structure for these two alloys. In the ordered state, the ferromagnetic spins of Ni atoms are probably frozen due to the process of ordering. Therefore, the Ni spins do not respond to magnetic field and we have consequently observed this unusual constant magnetic moment with magnetic field. Structural effects might also be considered in gaining an understanding of this anomaly.

(2) For the $x=0.35$ alloy, in the ordered state, at high magnetic field, a peak was observed near to T_c which indicates the tendency to change the magnetic moment from a ferromagnetic to an antiferromagnetic type. In the atomic phase diagram of the ordered structure, although the $x=0.35$ alloy exists in the $L1_2$ phase region, nevertheless the position is very near to the border line between $L1_2$ and $L1_0$ structures. The peak near T_c is probably due to that structural effect.

(3) For the $x=0.44$ alloy, in the disordered state, a ferromagnetic moment was observed for the whole range of magnetic field, although very peculiar results were observed in the ordered state. At 0- and 10-Oe magnetic field, a very weak ferromagnetic moment is observed, without any spontaneous magnetization. But at 50 Oe magnetic field, a weak antiferromagnetic peak appeared at 42 K with the coexistence of a weak ferromagnetic peak. Up to 800-Oe magnetic field, the antiferromagnetic moment increases and the ferromagnetic moment decreases with increasing magnetic field. At 1000-Oe magnetic field, a perfectly antiferromagnetic moment appears with complete disappearance of the weak ferromagnetic moment. Above 1200 Oe, only a paramagnetic moment is present with complete disappearance of the antiferromagnetic peak. Hysteresis-loop data and the negative value of the paramagnetic Curie temperature, Θ , confirmed the antiferromagnetic moment in the alloy, independently. But, it is difficult to give a theoretical interpretation of this peculiar magnetic phase change with magnetic field. Lower magnetic moment in the ordered state is responsible for the $L1_0$ layered structure. The present new data of magnetic phase transition with magnetic field for the $x=0.44$ alloy with help to establish new considerations in magnetism.

(4) For the $x=0.50$ alloy, a ferromagnetic moment was observed in the disordered state but a clear paramagnetic moment was observed in the ordered state for the whole magnetic-field range. Though a much lower magnetic moment was observed in the ordered state with the order of 10^{-6} emu/g, the moment still exists. Hysteresis-loop data and the value of Θ proved that the ordered state is perfectly paramagnetic for the $x=0.50$ alloy. $L1_0$ -type ordered structure is probably responsible for this type of change.

ACKNOWLEDGMENTS

The authors would like to express their thanks to S. Kim of University of Tsukuba for his help in measuring the SQUID data and Dr. E. Kita of University of Tsukuba and Dr. J. Inoue of Nagoya University for their helpful discussions.

- ¹V. V. Krishnamurthy, S. N. Mishra, M. R. Press, P. L. Paulose, S. H. Devare, and H. G. Devare, *Phys. Rev. B* **49**, 6726 (1994).
- ²C. D. Keener and M. B. Weissman, *Phys. Rev. B* **49**, 3944 (1994).
- ³P. A. Stampe, X. Chen, Z. Wang, H. P. Kunkel, and G. Williams, *J. Phys. Condens. Matter* **6**, 3045 (1994).
- ⁴M. C. Cadeville, C. E. Dahmani, and F. Kern, *J. Magn. Magn. Mater.* **54-57**, 1055 (1986).
- ⁵T. B. Massalski, H. Okamoto, and P. K. Subramanion, *Binary Alloy Phase Diagrams* (ASM International, Materials Park, 1990), Vol. 2, p. 1744.
- ⁶C. E. Dahmani, M. C. Cadeville, and V. P. Bohnes, *Acta Metall.* **33**, 369 (1985).
- ⁷W. B. Pearson, *A Handbook of Lattice Spacings and Structures of Metals and Alloys* (Pergamon, Oxford, 1958).
- ⁸D. K. Saha, K. Ohshima, M. Y. Wey, R. Miida, and T. Kimoto, *Phys. Rev. B* **49**, 15 715 (1994).
- ⁹P. Marchukov, R. Geick, C. Brotzeller, W. Treutmann, E. G. Rudashevsky, and A. M. Balbashov, *Phys. Rev. B* **48**, 13 538 (1993).